Journal of Marine Science and Technology

Volume 21 | Issue 3 Article 14

CASE STUDY OF ASIAN DUST EVENT ON MARCH 19-25, 2010 AND ITS IMPACT ON THE MARGINAL SEA OF CHINA

Fujung Tsai
Department of Marine Environmental Informatics, National Taiwan Ocean University, Keelung, Taiwan, R.O.C.,
fujung@mail.ntou.edu.tw

Yi-Shin Fang
Department of Marine Environmental Informatics, National Taiwan Ocean University, Keelung, Taiwan, R.O.C.

Shih-Jen Huang
Department of Marine Environmental Informatics, National Taiwan Ocean University, Keelung, Taiwan, R.O.C.

Recommended Citation
Tsai, Fujung; Fang, Yi-Shin; and Huang, Shih-Jen (2013) "CASE STUDY OF ASIAN DUST EVENT ON MARCH 19-25, 2010 AND ITS IMPACT ON THE MARGINAL SEA OF CHINA," *Journal of Marine Science and Technology*: Vol. 21: Iss. 3, Article 14.
DOI: 10.6119/JMST-013-0326-1
Available at: https://jmstt.ntou.edu.tw/journal/vol21/iss3/14

CASE STUDY OF ASIAN DUST EVENT ON MARCH 19-25, 2010 AND ITS IMPACT ON THE MARGINAL SEA OF CHINA

Acknowledgements

We extend our gratitude to Dr. Shih-Chieh Hsu for providing the aluminum data and to Dr. Jien-Yi Tu for the weather analysis data. The authors gratefully acknowledge the United States National Oceanic and Atmospheric Administration Air Resources Laboratory (ARL) for providing the Hybird Single-Particle Lagrangian Integrated Trajectory model taken from its website (http://www.arl.noaa.gov/ready.html) and used in this publication, and Dr. Nobuo Sugimoto in the National Institute for Environmental Studies in Japan for providing the Cape Hedo lidar data on the lidar network (http://www-lidar-nies.go.jp) for use in the publication. We also thanks the National Aeronautics and Space Administration for providing the Cloud-Aerosol Lidar and Infrared Pathfinder Satellite Observations data and the Moderate Resolution Imaging Spectroradiometer dataset as well as the Taiwan Central Weather Bureau for the World Meteorological Organization surface observation data used in our analysis. This study is supported by NSC 98-2611-M-019-019-MY3 project.

Journal of Marine Science and Technology, Vol. 21, No. 3, pp. 353-360 (2013)
DOI: 10.6119/JMST-013-0326-1

CASE STUDY OF ASIAN DUST EVENT ON MARCH 19-25, 2010 AND ITS IMPACT ON THE MARGINAL SEA OF CHINA

Fujung Tsai, Yi-Shin Fang, and Shih-Jen Huang

Key words: Asian dust event, dry deposition flux, soluble iron, chlorophyll-a.

ABSTRACT

This study analyzes the most severe dust event in Taiwan in the last 20 years. The dust event occurred from March 19 to 25, 2010, with PM_{10} (particular matter less than 10 μm) reaching a maximum beyond 1200 μg m^{-3}, and dust accounting for over 90% of the concentrations in Taiwan. The severe event originated from Mongolia on March 19, and the widespread dust moves southeastward toward Taiwan, with a thickness of 1 to 2 km near the ground. The concentrated dust layer can enhance phytoplankton bloom due to deposition of crustal nutrients, including iron. Over the marginal sea of China, the total deposition of soluble iron is estimated to be about 3926 μg m^{-2} during the event, and the chlorophyll-a concentrations over the East China Sea are enhanced by an average of approximately 0.6 mg m^{-3} and 1.5 mg m^{-3} in the first and second weeks, respectively, after the dust passage.

I. INTRODUCTION

Asian deserts are mainly located in Northwestern and Northern China, as well as in Mongolia, covering an area of around 600 thousand square kilometers. This region receives an annual rainfall of less than 400 mm, with an uneven seasonal distribution, resulting in the frequent occurrence of dust storms. From late winter to spring, especially from March to May, dust occurrence is frequently observed [18]. During this period, the desert is barely covered with plants. Therefore, when a cyclonic system passes through, dust event can be generated by the associated strong surface wind. The generated dust event can be transported downwind over thousands of kilometers. The transport pathways of Asian dust include eastward to the eastern coast of China, Korea, Japan, and even the North America, and southeastward to the East China Sea, Taiwan, and the South China Sea [33]. The transported dust can have notable effects on the downwind areas.

Aeolian dust can have a notable impact on atmospheric and oceanic conditions. The effects of dust on the atmosphere include both direct scattering and absorption of solar radiation [9, 37] and indirect effects related to dust's influence on cloud microphysics [27]. By acting as cloud condensation nuclei, dust can affect convective activity, cloud formation, and precipitation efficiency [2, 17, 20, 21, 30]. Dust particles influence the ocean because they contain crustal nutrients, such as iron, and are important to the marine biogeochemistry [6, 13, 22, 29]. The deposition of dust into the ocean enhances phytoplankton blooms and potentially leads to oceanic cooling through the absorption of more atmospheric carbon dioxide and the excretion of dimethyl sulfide by phytoplankton [31]. Through measurement, Zhang *et al*. [43] found that the decisive nutrient over the Pearl River estuary in East China is iron. Wang *et al*. [40] also found that the long-range transport of Asian dust has led to the rapid growth of phytoplankton in the South China Sea.

Taiwan is located off the eastern coast of Asia, and surrounded by the East China Sea in the north and the South China Sea in the south (Fig. 1). The island is located downwind of southeastward Asian dust events. In the past two decades, several dust events have reached the island every year, enhancing the atmospheric PM_{10} concentrations from less than 100 to 500 μg m^{-3} [18]. On March 21 to 25, 2010, a severe dust event was observed in Taiwan, where the PM_{10} level exceeded 1200 μg m^{-3}. The extreme PM_{10} level has not been observed during the past 20 years. In addition, the high dust concentration was also observed in southern Taiwan, unlike previous events that are mostly observed in Northern Taiwan. To understand the generation and the impacts of the extreme dust event on the marginal sea of China, we analyze the dust related observation obtained from surface stations in Taiwan. In addition, trajectory and weather analyses are applied to assess the source and transport of the dust event. Dust and iron deposition fluxes over the marginal sea are calculated and the enhancement of the phytoplankton due to the dust

Paper submitted 01/25/13; revised 03/11/13; accepted 03/26/13. Author for correspondence: Fujung Tsai (e-mail: fujung@mail.ntou.edu.tw).
Department of Marine Environmental Informatics, National Taiwan Ocean University, Keelung, Taiwan, R.O.C.

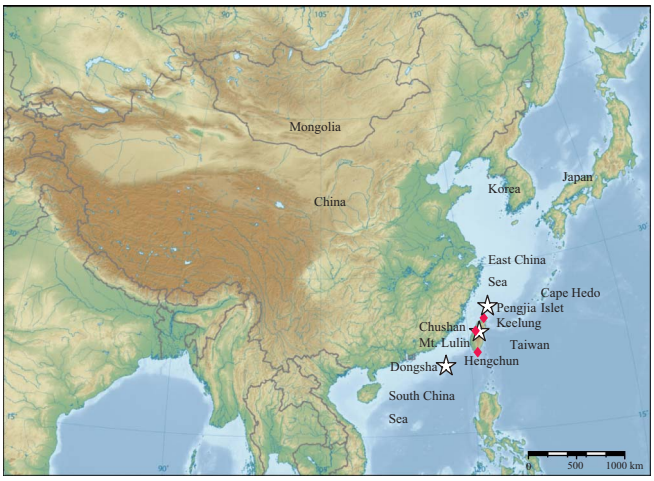

Fig. 1. Map of East Asia, the ground measurements from Pengjia Islet, Mt. Lulin, and Dongsha Atoll (white star), the Taiwan EPA surface stations, including Keelung, Chushan and Hengchun (red dot), and the lidar measurement from Cape Hedo, Japan.

passage is quantified through analyzing the chlorophyll-a concentration obtained via satellite.

II. DATA AND METHODS

1. Surface Observations

Two types of surface observation are used. First, the daily aluminum (Al) mass in the PM_{10} particles is obtained from three ground stations, namely, Pengjia Islet, Mt. Lulin, and Dongsha Atoll (Fig. 1), and is used for deriving dust mass. Second, the hourly aerosol concentrations including PM_{10} and $PM_{2.5}$ (particulate matter less than 2.5 um) are obtained from the Taiwan Environmental Protection Administration (EPA), namely, Keelung, Chushan, and Hengchun stations (Fig. 1). As these EPA stations with aerosol observations are the closest sites to the three ground stations with Al measurements, the observed aerosol concentrations can be used to compare with the dust concentration derived from Al measurements.

Al is a crustal element, not usually associated with an anthropogenic source [e.g., 41]. It has been used as an index of dust in previous studies [e.g., 7, 38]. Al usually accounts for 6 to 8% of bulk dust mass [23, 35, 36, 44], and this ratio remains almost unchanged during transport. Therefore, following previous studies, this study use 8% in deriving Al mass into dust concentrations [11]. The Al element in PM_{10} samples is analyzed by using inductively coupled plasma mass spectrometry (ICP-MS), with a detection limit of 2ng m^{-3}. Details of the methodology can be found in the study by Hsu *et al*. [11].

2. Lidar

The lidar measurements at Cape Hedo (128.25°E, 26.87°N) are obtained from the website of the National Institute for Environmental Studies in Japan (http://www-lidar.nies.go.jp/). Both aerosol backscattering (532 nm and 1064 nm) and depolarization (at 532 nm) are measured with a laser power of 30 mJ and 20 mJ, respectively, for both wavelengths, with a repetition rate of 10 Hz, and a telescope diameter of 20 cm. The height resolution is 6 m.

In addition to the ground measurement, lidar on board the satellite is also used to identify the dust event. The United States National Aeronautics and Space Administration (NASA) Cloud-Aerosol Lidar and Infrared Pathfinder Satellite Observations (CALIPSO) measured the vertical distribution of aerosols in the atmosphere as well as their optical and physical properties.

The lidar depolarization ratio and extinction coefficient are used to identify the aerosol particles in the atmosphere. The depolarization ratio is the ratio of the vertical direction of the polarized light to the parallel direction of the polarized light. A greater value of depolarization ratio is obtained when the particle is more irregular. The depolarization ratio varies greatly among different aerosol particles. For example, the depolarization ratio is about 2% in dry sulfate crystals, 5 to 30% in Asian dust, 6 to 11% in biomass burning, and 8 to 22% in sea salt. On the other hand, the extinction coefficient is related to the absorption or scattering (such as back scattering) of aerosol in the atmosphere, and thus can be used to retrieve aerosol profile in the atmosphere. The dust extinction obtained from Cape Hedo is derived from total extinction and depolarization ratio of aerosol particles. The method for deriving the dust extinction can be referred to Shimizu *et al*. (2004) and Sugimoto *et al*. (2008).

3. Trajectory

The path of an individual small air parcel traveling through space and time can be calculated by using a trajectory model. In this study, the United States National Oceanic and Atmospheric Administration (NOAA) Air Resources Laboratory (ARL) Hybrid Single-Particle Lagrangian Integrated Trajectory (HYSPLIT) model from the website (http://www.arl.noaa.gov/HYSPLIT_info.php) is used in calculating the backward trajectory of an air parcel containing dust [5] (version 4). The model has been widely applied in prior studies to examine the source of the dust events [3, 15, 19, 26, 39]. The meteorological input for calculating the trajectory of the model is obtained from the GDAS (Global Data Assimilation System) output [4, 24, 25].

The trajectory of this study is initiated from the Pengjia Islet (122.07°E, 25.63°N), the northernmost station in Taiwan, and traced back for several days. The initial time is determined to be four hours before and after the occurrence of the peak PM_{10} concentrations observed in Taiwan. The initial height determined from lidar measurements ranges from 300 to 3000 m, and one trajectory is plotted for every 100 m in this range. A total of 500 trajectories are obtained. Trajectories that do not pass through the deserts are neglected, as these air parcels can originate from other sources and contain no dust particles. The selected trajectories are classified according

to their path and then compared with surface observation of dust activities in order to determine their source locations. As most of these trajectories originate from almost the same source locations, only one representative trajectory is selected for discussion.

4. Weather Analysis

The National Centers for Environmental Prediction (NCEP)-National Center for Atmospheric Research (NCAR) Reanalysis [14] is used for analyzing the synoptic conditions during the dust event. The global reanalysis data has a spatial resolution of 2.5° × 2.5° and a temporal resolution of 6 hours, including surface wind field and sea-level pressure.

Dust observations from surface stations in East Asia are obtained for analyzing dust event. From World Meteorological Organization (WMO), the present weather observation includes dust activities of different intensities [42]. The observation codes from 6 to 9 represent dust intensities from haze to severe dust storm, and 30 to 35 represent different intensities of severe dust storm. Both codes are employed to identify dust events.

5. Satellite Image

The sea surface chlorophyll-a concentration is obtained from the National Aeronautics and Space Administration (NASA) as part of the Moderate Resolution Imaging Spectroradiometer (MODIS) Terra Level-3 dataset [16]. The MODIS instruments are onboard the NASA Earth Observing System (EOS) Terra satellites [1, 28]. Eight-day composite chlorophyll-a concentrations are used, with a resolution of 9 km.

III. RESULTS

Fig. 2 compares the temporal variations of the derived dust concentration from ground measurements with the observed PM_{10} and $PM_{2.5}$ concentrations, and their ratio obtained from the closest EPA stations from north to south of Taiwan. Fig. 2(a) shows the enhanced PM_{10} concentration of 1228 μg m^{-3} observed at the Keelung station on March 21 when the dust event is passing over northern Taiwan. The extreme PM_{10} concentration indicates the upcoming of an extremely strong dust event that was not seen during the past 20 years. At the same time, the $PM_{2.5}$ concentrations also reach about 250 μg m^{-3}, a extremely high value in the record of the history. Similarly, the ratios of PM_{10} to $PM_{2.5}$ increase. As dust particles are usually larger in size, the high ratio indicates the arrival of dust particles instead of other smaller particles, such as pollutants. Furthermore, the daily dust concentrations derived from the Pengjia Islet nearby the Keelung station reaches 638 μg m^{-3} on the same day, confirming the arrival of dust event. As PM_{10} includes both anthropogenic pollutants and dust, to quantify the dust concentration, the derived dust concentration from Al is used, as in previous studies [e.g., 7, 38]. Because the Pengjia Islet is located close to the Keelung

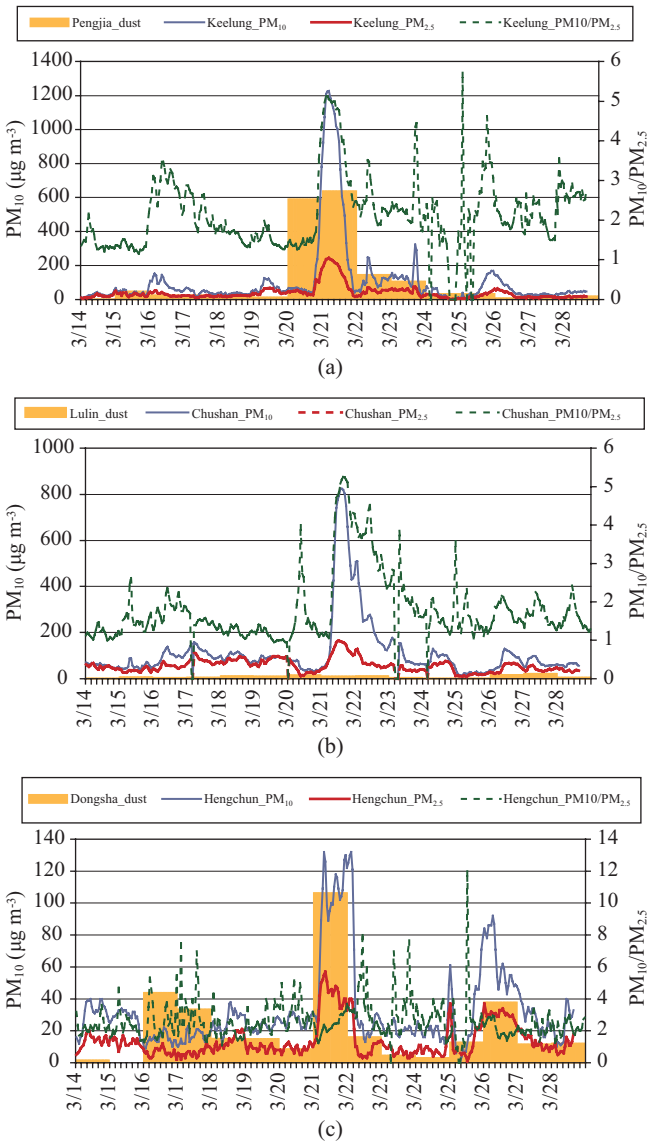

Fig. 2. Dust concentrations (use PM_{10} axis) from ground measurements of (a) Pengjia Islet, (b) Mt. Lulin, and (c) Dongsha Atoll, and the observed PM_{10}, $PM_{2.5}$ (use PM_{10} axis) concentrations and their ratio from the closest EPA stations, such as Keelung, Chushan, and Hengchun, respectively.

station, the dust fraction in PM_{10} particles during the dust event on March 21 can be estimated through averaging the daily PM_{10} concentration in Keelung (700 μg m^{-3}) and compares with the daily dust concentration at Pengjia Islet (638 μg m^{-3}). Through the calculation, we found that dust has accounted for approximately 90% of observed PM_{10} concentration in Keelung or northern Taiwan during this event.

The PM_{10} concentrations decrease rapidly to about 800 μg m^{-3} in Central Taiwan (Fig. 2(b)), and 130 μg m^{-3} in Southern Taiwan (Fig. 2(c)) on the same day, with a slight time lag due to distance. In Central Taiwan, although high PM_{10} concentrations are measured in the EPA surface station, little dust concentrations are observed at the nearby Mt. Lulin

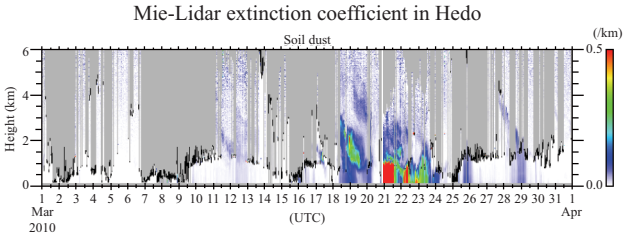

Fig. 3. Mie-Lidar extinction coefficient showing vertical distribution of dust on March 21-23, 2010 at Cape Hedo.

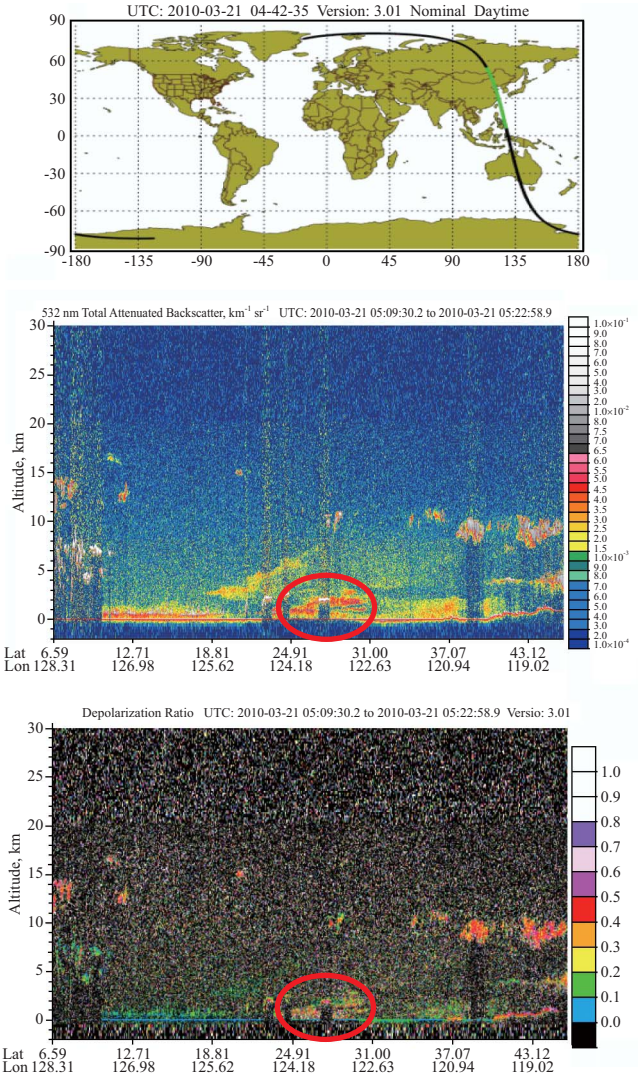

Fig. 4. NASA Cloud-Aerosol Lidar and Infrared Pathfinder Satellite Observations of their path (top) and vertical distribution of backscattering (middle) and depolarization ratio (bottom) on March 21. The period when satellite passed through Taiwan and the nearby areas are circled.

station, which has an altitude of about 2.9 km. It implies that the dust event travels within a thin layer on the surface. In the southern stations, the derived dust concentrations are around 100 μg m^{-3} at Dongsha, similar to the observed PM_{10}

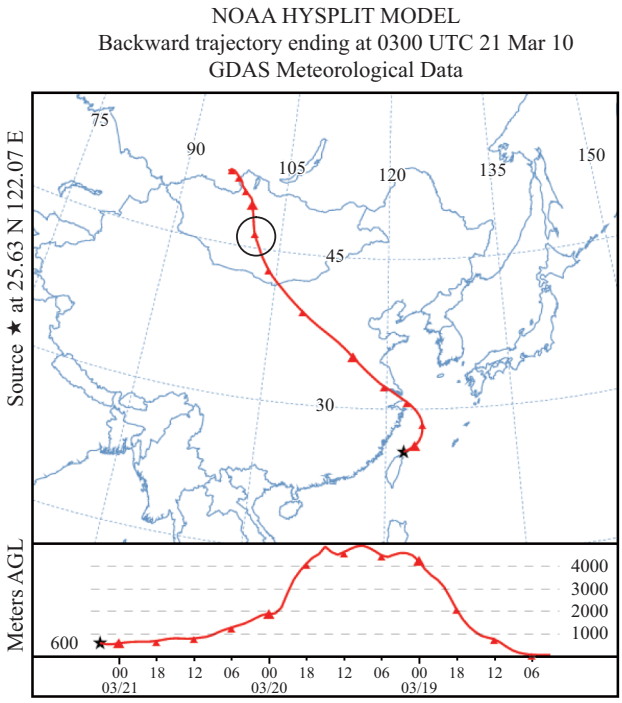

Fig. 5. NOAA HYSPLIT trajectory showing the path and height of the dust loaded air parcel arriving Taiwan originates from Mongolia. The location and time of dust generation is circled.

concentrations at Hengchun. As Hengchun is located to the north of Dongsha, the dust concentration at Hengchun is expected to be at least the same as that in Dongsha during southward transport of dust event. Thus, the same values of PM_{10} and dust concentrations in Hengchun (100 μg m^{-3}) indicate that dust accounts for nearly 100% of the aerosol concentration in southern Taiwan.

Fig. 3 shows the ground measurements of lidar from Cape Hedo obtained during the dust event. The measurement of extinction coefficient demonstrates that the maximum height of the dust event remains predominately at 1 to 2 km above the ground on March 21-23. Similarly, the lidar measurement of depolarization ratio from CALIPSO also shows that the dust distributions are mainly concentrated within 1 to 2 km near the surface when it passes through Taiwan and the neighboring marine areas (Fig. 4). Both lidar measurements imply that the extraordinarily high dust event are concentrated in a thin layer near the surface.

The HYSPLIT backward trajectory model is applied in identifying the source location of the dust event. The result shows that the dust-loaded air parcel arriving in Northern Taiwan passes through Mongolia on March 19 (Fig. 5). As the air parcel moves across Mongolia at 06 UTC on March 19, dust activity is also detected by the ground station right below the air parcel (Fig. 6). According to the vertical distribution of the trajectory, the dust particle is likely lifted up to a height of about 4 km above the ground (Fig. 5) under strong surface mixing during the dust event, which often can

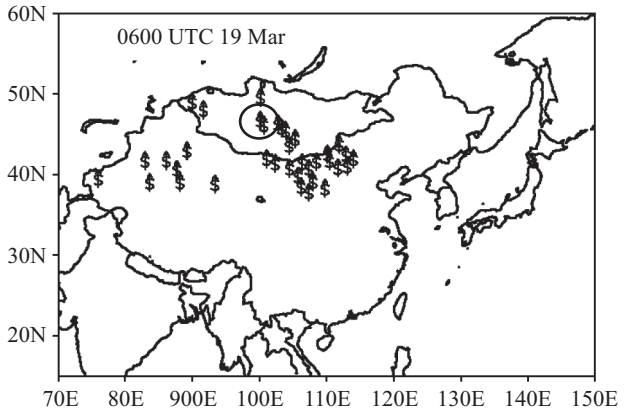

Fig. 6. Dust observation from surface stations obtained from WMO at 0600 UTC on March 19. Black circle shows the location of dust generation that matches the path of backward trajectory in Fig. 5.

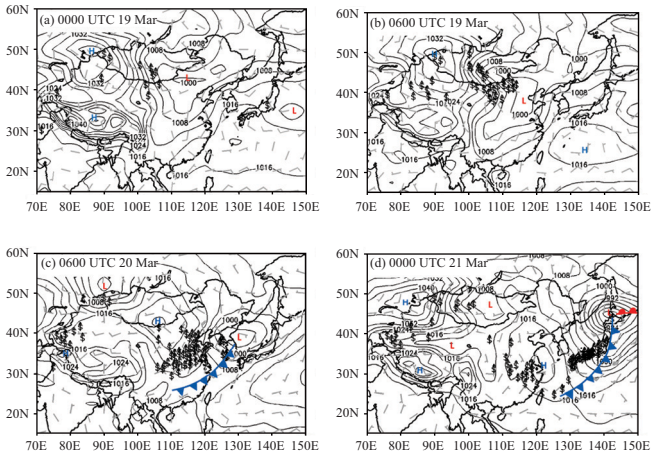

Fig. 7. Surface weather map of dust event at (a) 0000 UTC March 19, (b) 0600 UTC March 19, (c) 0600 UTC March 20, and (d) 0000 UTC March 21, 2001. High (H) and Low (L) pressure systems, cold (blue triangle) and warm (red semicircle) fronts, and surface dust observations ($) are marked. Full barb and half barb represent wind velocity of 10 ms^{-1} and 5 ms^{-1}.

not be simulated in the trajectory model. The dust parcel then advected downwind following the path of the trajectory.

Besides trajectory, the synoptic weather map with dust observations from surface stations in China is also used in verifying the transport of dust event downwind to Taiwan. Fig. 7 shows that strong winds brought by the intense pressure gradient initiated dust event in Mongolia at 0000 UTC to 0600 UTC on March 19 (Fig. 7(a)-(b)). The intense dust observations from surface stations reveal that the extremely severe dust event covering a wide area of Mongolia and China. Subsequently, the dust event moves southeastward downwind following the movement of the surface front. The dust event passes over the East China Sea and Northern Taiwan on March 20 to 21 (Figs. 7(c)-(d)). Since the anticyclonic circulation only passes through northern Taiwan, significant amount of dust follows the circulation and arrives

Table 1. Daily dust concentrations, calculated dry deposition flux of dust and soluble iron during the passage of the dust event over the East China Sea.

Dust Concentration ($\mu g\ m^{-3}$)	Month/date	Dust Deposition flux ($\mu g\ m^{-2}s^{-1}$)	Soluble iron deposition flux ($\mu g\ m^{-2}\ day^{-1}$)
590	03/20	12	1451
639	03/21	14	1693
147	03/22	3	356
107	03/23	2	259
34	03/24	1	82
35	03/25	1	85

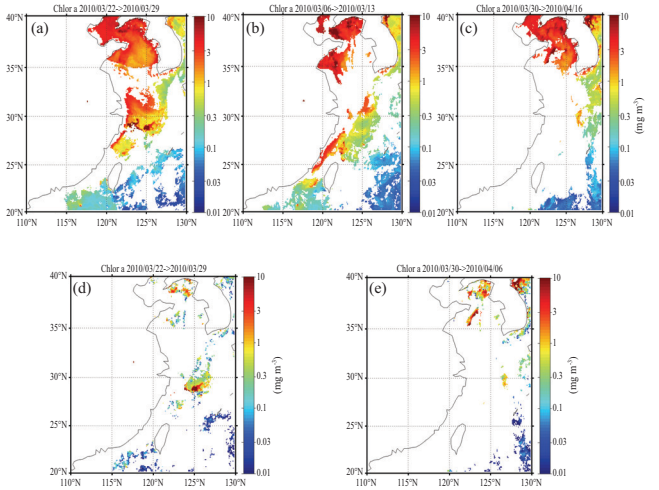

Fig. 8. Eight-day composite chlorophyll-a concentrations from MODIS (a) before and (b)-(c) after the dust event on March 21, and (d)-(e) their differences due to dust passage over the marginal sea of China.

at northern Taiwan. Due to the limitation of the circulation, the dust concentrations decrease rapidly with distance toward southern Taiwan, reaching about 100 $\mu g\ m^{-3}$ (Fig. 2(c)), which is still extremely high compared to the values in southern Taiwan in previous dust events. The passage of the dust event with high dust concentrations can significantly affect the marine biogeochemistry through dust deposition.

The depositions of the dust particles over the marginal sea of China are calculated. Dust depositions are obtained from dust concentration and deposition velocity. We estimate the dust deposition over the East China Sea by taking the dust concentrations observed on the Pengjia Islet as the representative value for the East China Sea. By multiplying the dry deposition velocity of 2 cm s^{-1} measured from Hsu *et al.*, [10], the dust depositions over the East China Sea are obtained. As soluble iron is the chemical species of a dust particle that can be uptake by phytoplankton, we calculate the soluble iron in dust particles by assuming that iron accounts for 3.5% of dust mass, and the proportion of soluble iron to

be 4% of the total iron, as in previous studies [10, 44]. The results are summarized in Table 1.

As shown in Table 1, the dust concentration on the Pengjia Islet varies from 35 to 639 μg m^{-3} during the dust event from March 20 to 25. In multiplying the deposition velocity, the estimated dust deposition flux ranges from 1 to 14 μg $m^{-2}s^{-1}$, and the deposition flux of soluble iron varies from less than a 100 to about 1700 μg m^{-2} day^{-1}, with a total of 3926 μg m^{-2} during the severe dust event. The maximum daily deposition flux of soluble iron obtained on March 21 is 40 times greater than the daily averaged value to the East China Sea in spring [12].

The high deposition flux due to the passage of the dust event is expected to enhance phytoplankton bloom. Fig. 8 shows the eight-day composite chlorophyll-a image over the marginal sea of China obtained from MODIS. The distribution of the chlorophyll-a concentrations varies from less than 0.01 to over 10 mg m^{-3} as the concentration moves toward the continent (Figs. 8(a)-(c)). The eight-day composite concentration on March 6-13 is used to represent the value before the dust event, and the enhancement in the chlorophyll-a are calculated by subtracting the concentrations before the dust event from the concentration one and two weeks after the dust event. The results show that over 3 mg m^{-3} of chlorophyll-a is enhanced over several areas of the East China Sea during the first week of dust passage, and this enhancement decreases over the East China Sea during the second week of dust passage, but increases over the Yellow Sea, located north of the East China Sea (Figs. 8(d)-(e)). By averaging the values over the whole area, the calculated chlorophyll-a enhancement is found to be about 0.65 during the first week and 1.54 mg m^{-3} during the second week. These values are comparable with those in previous studies [8]. The effective grid numbers are over 2000 in both two weeks in the 9 km resolution of the satellite image. These results confirm the impacts of the dust event on the phytoplankton bloom over the East China Sea.

IV. CONCLUSION

We analyze the severe dust event on March 19 to 25, 2010 using surface observation data, backward trajectory model, and weather analysis. The effects of the event due to dust depositions are calculated and the enhancement of chlorophyll-a from satellite image are quantified. Dust observations show that the event covers the whole island of Taiwan, with observed PM_{10} concentration exceeding 1200 μg m^{-3} in Northern Taiwan, 800 μg m^{-3} in Central Taiwan, and 130 μg m^{-3} in southern Taiwan. Using the measured aluminum mass in PM_{10} particles, the dust concentrations in PM_{10} particles over Taiwan are derived. The result indicates that the dust concentrations account for over 90% of the background atmospheric PM_{10} concentrations over Taiwan during the passage of the event.

The backward trajectory, weather analyses, and surface dust observation suggest that the dust event originates from Mongolia on March 19 because of the strong winds generated by an intense pressure gradient. Then, the dust event moves downwind ahead of the high-pressure system and passes through the East China Sea and Taiwan on March 21 to 25. Since the anticyclonic circulation only passes through northern Taiwan, significant amount of dust follows the circulation and arrives at northern Taiwan, but the concentration decreases rapidly with distance toward southern Taiwan. According to lidar and ground measurements, the dust-loaded air mass swept through Taiwan and the marginal sea with a thickness of 1 to 2 km near the ground.

Concentrated dust particles moving near the surface layer can significantly affect marine biogeochemistry due to deposition of crustal nutrients, including iron. As soluble iron is the iron species that can be uptake by phytoplankton, the dry deposition flux of soluble iron is quantify by multiplying the dust concentration obtained from the Pengjia Islet, by the dry deposition velocity and the fraction of the soluble iron in a dust particle. The total deposition of the soluble iron from the event is estimated to be about 3926 μg m^{-2} and a daily maximum of 1693 μg $m^{-2}day^{-1}$ over the East China Seas. The daily maximum flux is forty times greater than the regular dust depositions over the area in spring [12].

The chlorophyll-a concentrations from MODIS are used to quantify the change in phytoplankton over the marginal sea of China after the dust passage. The results indicate that the severe dust event increases the chlorophyll-a concentration of about 0.6 to 1.5 mg m^{-3} over the East China Sea. The enhanced concentration can be contributed from dry deposition of crustal nutrients, such as soluble iron. It is also possible that the enhancement is contributed from other factors, such as mixing of the sea surface water initiated by strong surface wind during dust passage, through which nutrients are likely carried upward to the sea surface layer resulting in enhancement of phytoplankton bloom. Further studies are needed to quantify the contribution of chlorophyll-a enhancement from different mechanism.

ACKNOWLEDGMENTS

We extend our gratitude to Dr. Shih-Chieh Hsu for providing the aluminum data and to Dr. Jien-Yi Tu for the weather analysis data. The authors gratefully acknowledge the United States National Oceanic and Atmospheric Administration Air Resources Laboratory (ARL) for providing the Hybird Single-Particle Lagrangian Integrated Trajectory model taken from its website (http://www.arl.noaa.gov/ready.html) and used in this publication, and Dr. Nobuo Sugimoto in the National Institute for Environmental Studies in Japan for providing the Cape Hedo lidar data on the lidar network (http://www-lidar-nies.go.jp) for use in the publication. We also thanks the National Aeronautics and Space Administration for providing the Cloud-Aerosol Lidar and Infrared Pathfinder Satellite Observations data and the Moderate Resolution Imaging Spectroradiometer dataset as well as the

Taiwan Central Weather Bureau for the World Meteorological Organization surface observation data used in our analysis. This study is supported by NSC 98-2611-M-019-019-MY3 project.

REFERENCES

1. Barnes, W. L., Pagano, T. S., Salomonson, V. V., Directorate, E. S., Center, N., and Greenbelt, M. D., "Prelaunch characteristics of the moderate resolution imaging spectroradiometer (MODIS) on EOS-AM1," *IEEE Transactions on Geoscience and Remote Sensing*, Vol. 36, No. 4, pp. 1088-1100 (1998).
2. Bryson, R. A. and Barreis, D. A., "Possibilities of major climatic modifications and their implications: northwest India, a case for study," *Bulletin of the American Meteorological Society*, Vol. 48, pp. 136-142 (1967).
3. Cabello, M., Orza, J. A. G., Barrero, M. A., Gordo, E., Berasaluce, A., Cantón, L., Dueñas, C., Fernández, M. C., and Pérez, M., "Spatial and temporal variation of the impact of an extreme Saharan dust event," *Journal of Geophysical Research*, Vol. 117, No. D11, DOI: 10.1029/2012JD017513 (2012).
4. Derber, J. C., Parrish, D. F., and Lord, S. J., "The new global operational analysis system at the National Meteorological Center," *Weather and Forecasting*, Vol. 6, pp. 538-547 (1991).
5. Draxler, R. R. and Hess, G. D., "Description of the HYSPLIT-4 modeling system," *NOAA Technical Memorandum ERL ARL-224* (1997).
6. Duce, R. A. and Tindale, N. W. "Atmospheric transport of iron and its deposition in the ocean," *Limnology and Oceanography*, Vol. 36, No. 8, pp. 1715-1726 (1991).
7. Duce, R. A., Unni, C. K., Ray, B. J., Prospero, J. M., and Merrill, J. T., "Long-range atmospheric transport of soil dust from Asia to the tropical North Pacific: Temporal variability," *Science*, Vol. 209, pp. 1522-1524 (1980).
8. Gong, G.-C. and Liu, G.-J., "An empirical primary production model for the East China Sea," *Continental Shelf Research*, Vol. 23, No. 2., pp. 213-224 (2003).
9. Haywood, J. and Boucher, O., "Estimates of the direct and indirect radiative forcing due to tropospheric aerosols: A review," *Reviews of Geophysics*, Vol. 38, pp. 513-543, DOI: 10.1029/1999RG000078 (2000).
10. Hsu, S. C., Liu, S. C., Arimoto, R., Liu, T., Huang, Y., Tsai, F., Lin, F., and Kao, S., "Dust deposition to the East China Sea and its biogeochemical implications," *Journal of Geophysical Research*, Vol. 114, D15304, DOI: 10.1029/2008JD011223 (2009).
11. Hsu, S. C., Liu, S. C., Huang, Y. T., Lung, C. S., Tsai, F., Tu, J.-Y., and Kao, S. J., "A criterion for identifying Asian dust events based on Al concentration data collected from northern Taiwan between 2002 and early 2007," *Journal of Geophysical Research*, Vol. 113, D18306, DOI: 10.1029/2007JD009574 (2008).
12. Hsu, S. C., Wong, G. T. F., Gong, G. C., Shiah, F.-K., Huang, Y.-T., Kao, S.-J., Tsai, F., Lung, S.-C. C., Lin, F.-J., Lin, I.-I., Hung, C.-C., and Tseng, C.-M., "Sources, solubility, and dry deposition of aerosol trace elements over the East China Sea," *Marine Chemistry*, Vol. 120, pp. 116-127 (2010).
13. Jickells, T. D., Dorling, S., Deuser, W. G., Church, T. M., Arimoto, R., and Prospero, J. M., "Air-borne dust fluxes to a deep water sediment trap in the Sargasso Sea," *Global Biogeochemical Cycles*, Vol. 12, pp. 311-320 (1998).
14. Kalnay, E., Kanamitsu, M., Kistler, R., Collins, W., Deaven, D, Gandin, L., Iredell, M, Saha, S., White, G., Woollen, J., Zhu, Y., Chelliah, M., Ebisuzaki, W., Higgins, W., Janowiak, J., Mo, K. C., Ropelewski, C., Wang, J., Leetmaa, A., Reynolds, R., Jenne, R., and Joseph, D., "The NCEP/NCAR 40-year reanalysis project," *Bulletin of the American Meteorological Society*, Vol. 77, No. 3, pp. 437-471 (1996).
15. Lee, Y. C., Yang, X., and Wenig, M., "Transport of dusts from East Asian and non-East Asian sources to Hong Kong during dust storm related events 1996-2007," *Atmospheric Environment*, Vol. 44, pp. 3728-3738 (2010).
16. Letelier, R. M. and Abbott, M. R., "An analysis of chlorophyll fluorescence algorithms for the moderate resolution imaging spectrometer (MODIS)," *Remote Sensing of Environment*, Vol. 58, No. 2, pp. 215-223 (1996).
17. Levy, Y. and Rosenfeld, D., "Ice nuclei, rainwater chemical composition, and Static Cloud Seeding Effects in Israel," *Journal of Applied Meteorology*, Vol. 35, pp. 1494-1501 (1996).
18. Liu, T.-H., Tsai, F., Hsu, S.-C., Hsu, C.-W., Shiu, C.-J., Chen, W.-N., and Tu, J.-Y., "Southeastward transport of Asian dust: Source, transport and its contributions to Taiwan," *Atmospheric Environment*, Vol. 43, No. 2, pp. 458-467, DOI: 10.1016/j.atmosenv.2008.07.066 (2009).
19. Logan, T., Xi, B., Dong, X., Obrecht, R., Li, Z., and Cribb, M., "A study of Asian dust plumes using satellite, surface, and aircraft measurements during the INTEX-B field experiment," *Journal of Geophysical Research*, Vol. 115, D00K25, DOI: 10.1029/2010JD014134 (2010).
20. Lohmann, U. and Feichter, J., "Global indirect aerosol effects: A review," *Atmospheric Chemistry and Physics*, Vol. 5, pp. 715-737, DOI: 10.5194/acp-5-715-2005 (2005).
21. Maley, J., "Dust, clouds, rain types and climatic variations in tropical north Atlantic," *Quaternary Research*, Vol. 18, pp. 1-6 (1982).
22. Martin, J. H., Gordon, R. M., and Fitzwater, S. E., "The case for iron," *Limnology and Oceanography*, Vol. 36, pp. 1793-1802 (1991).
23. Nishikawa, M., Hao, Q., and Morita, M., "Preparation and evaluation of certified reference materials for Asian mineral dust," *Global Environmental Research*, Vol. 4, pp. 103-113 (2000).
24. Parrish, D. F. and Derber, J. C., "The National Meteorological Center's spectral statistical-interpolation analysis system," *Monthly Weather Review*, Vol. 120, pp. 1747-1763 (1992).
25. Petersen, R. A. and Stackpole, J. D., "Overview of the NMC production suite," *Weather and Forecasting*, Vol. 4, pp. 313-322 (1989).
26. Prasad, A. K. and Singh, R. P., "Changes in aerosol parameters during major dust storm events (2001-2005) over the Indo-Gangetic Plains using AERONET and MODIS data," *Journal of Geophysical Research*, Vol. 112, D09208, DOI: 10.1029/2006JD007778 (2007).
27. Rosenfeld, J. E., Considine, D. B., Meade, P. E., Bacmeister, J. T., Jackman, C. H., and Schoeberl, M. R., "Stratospheric effects of Mount Pinatubo aerosol studied with a coupled two-dimensional model," *Journal of Geophysical Research*, Vol. 102, pp. 3649-3670 (1997).
28. Salomonson, V. V., Barnes, W. L., Maymon, P. W., Montgomery, H. E., and Ostrow, H., "MODIS advanced facility instrument for studies of the Earth as a system," *IEEE Transactions on Geoscience and Remote Sensing*, Vol. 27, pp. 145-153 (1989).
29. Sarthou, G., Baker, A. R., Blain, S., Achterberg, E. P., Boye, M., Bowie, A. R., Croot, P., Laan, P., de Baar, H. J. W., Jickells, T. D., and Worsfold, P. J., "Atmospheric iron deposition and sea-surface dissolved iron concentrations in the eastern Atlantic Ocean," *Deep Sea Research I*, Vol. 50, pp. 1339-1352 (2003).
30. Sassen, K., "Indirect climate forcing over the western US from Asian dust storms," *Geophysical Research Letter*, Vol. 29, DOI: 10.1029/2001GL014051 (2002).
31. Schollaert, S. E. and Merrill, J. T., "Cooler sea surface west of the Sahara Desert correlated to dust events," *Geophysical Research Letters*, Vol. 25, pp. 3529-3532 (1998).
32. Shimizu, A., Sugimoto, N., Matsui, I., Arao, K., Uno, I., Murayama, T., Kagawa, N., Aoki, K., Uchiyama, A., and Yamazaki, A., "Continuous observations of Asian dust and other aerosols by polarization lidars in China and Japan during ACE-Asia," *Journal of Geophysical Research*, Vol. 109, D19S17, DOI: 10.1029/2002JD003253 (2004).
33. Sugimoto, N., Matsui, I., Shimizu, A., and Nishizawa, T., "Lidar network for monitoring Asian dust and air pollution aerosols," *IEEE International Geoscience & Remote Sensing Symposium*, Boston, Massachusetts, pp. 573-576 (2008).
34. Sun, J., Zhang, M., and Liu, T., "Spatial and temporal characteristics of dust storms in China and its surrounding regions, 1960-1999: Relations to source area and climate," *Journal of Geophysical Research*, Vol. 106, pp. 10325-10334 (2001).

35. Sun, Y., Zhuang, G., Wang, Y., Zhao, X., Li, J., Wang, Z., and An, Z., "Chemical composition of dust storms in Beijing and implications for the mixing of mineral aerosol with pollution aerosol on the pathway," *Journal of Geophysical Research*, Vol. 110, DOI: 10.1029/2005JD006054 (2005).
36. Taylor, S. R., "Abundance of chemical elements in the continental crust: a new table," *Geochimica et Cosmochimica Acta*, Vol. 28, pp. 1273-1285 (1964).
37. Tegen, I., Lacis, A. A., and Fung, I., "The influence on climate forcing of mineral aerosols from disturbed soils," *Nature*, Vol. 380, No. 6573, pp. 419-422 (1996).
38. Uematsu, M., Duce, R. A., Merrill, J. T., Chen, L., Prospero, J. M., and McDonald, R. L., "Transport of mineral aerosol from Asia over the North Pacific Ocean," *Journal Geophysical Research*, Vol. 88, pp. 5343-5352 (1983).
39. Vishkaee, F. A., Flamant, C., Cuesta, J., Flamant, P., and Khalesifard, H. R., "Multiplatform observations of dust vertical distribution during transport over northwest Iran in the summertime," *Journal of Geophysical Research*, Vol. 116, D05206, DOI: 10.1029/2010JD014573 (2011).
40. Wang, S.-H., Hsu, N. C., Tsay, S.-C., Lin, N.-H., Sayer, A. M., Huang, S.-J., and Lau, W. K. M., "Can Asian dust trigger phytoplankton blooms in the oligotrophic northern South China Sea?" *Geophysical Research Letters*, Vol. 39, No. 5, DOI: 10.1029/2011GL050415 (2012).
41. Windom, H. L., Schropp, S. J., Calder, F. D., Ryan, J. D., Smith, R. Q. Jr., Burney, L. C., Lewis, F. Q., and Rawllnson, C. H., "Natural trace metal concentrations in estuarine and coastal marine sediments of the south-eastern United States," *Environmental Science Technology*, Vol. 23, No. 3, pp. 314-320 (1989).
42. World Meteorological Organization (WMO), *Manual on the Global Observing System, Volume I, Global Aspects*, WMO No. 544, 2010, http://www.wmo.int/pages/prog/www/OSY/Manuals_GOS.html.
43. Zhang, J., Yu, Z. G., Wang, J. T., Ren, J. L., Chen, H. T., Xiong, H., Dong L. X., and Xu, W. Y., "The subtropical Zhujiang (Pearl River) estuary: nutrient, trace species and their relationship to photosynthesis," *Estuarine, Coastal and Shelf Science*, Vol. 49, pp. 385-400 (1999).
44. Zhang, X. Y., Arimoto, R., and An, Z. S., "Dust emission from Chinese desert sources linked to variations in atmospheric circulation," *Journal of Geophysical Research*, Vol. 102, No. D23, pp. 28041-28047 (1997).
45. Zhang, X. Y., Gong, S. L., Shen, Z. X., Mei, F. M., Xi, X. X., Liu, L. C., Zhou, Z. J., Wang, D., Wang, Y. Q., and Cheng, Y., "Characterization of soil dust aerosol in China and its transport and distribution during 2001 ACE-Asia: 1. Network observations," *Journal of Geophysical Research*, Vol. 108, pp. 8032-8039 (2003).